

INVESTIGATION OF OSB THICKNESS-SWELL BASED ON A 3D DENSITY DISTRIBUTION. PART I. THE FINITE ELEMENT MODEL

Alan D. Tackie

Engineer
OPUS Architects and Engineers
10350 Bren Road West
Minnetonka, MN 55343

Siqun Wang[†]

Associate Professor
Tennessee Forest Products Center
The University of Tennessee
2506 Jacob Dr.
Knoxville, TN 37996-4563

Richard M. Bennett

Professor
221 Perkins Hall
Department of Civil & Environmental Engineering
The University of Tennessee
Knoxville, TN 37996-2010

and

Sheldon Q. Shi[†]

Assistant Professor
Department of Forest Products
P. O. Box 9820
Mississippi State University
Mississippi State, MS 39762-9820

(Received June 2006)

ABSTRACT

A finite element model was developed for predicting thickness-swell of oriented strandboard. The model accounts for both vertical and horizontal density variations of the board, or the three-dimensional density distribution. Density variation, resulting from manufacturing processes such as strand orientation and pressing cycles, affects the uniformity of thickness-swell in OSB. The model uses nonlinear constitutive behavior in the through-the-thickness direction. Moisture changes were modeled using transient moisture transfer equations and coupled moisture-density-stress-strain relations. The model was used to predict thickness-swell during a 24-h soak test. The model was able to predict average thickness-swell of commercial panels with an acceptable error, generally less than 10%.

Keywords: Thickness-swell, OSB, modeling, density distribution, VDP, HDD.

[†] Member of SWST

INTRODUCTION

Oriented strandboard (OSB) is a complex wood composite that has a non-uniform density distribution in both the through-the-thickness (vertical) direction and in the in-plane (horizontal) directions. The three-dimensional density distribution affects many properties that influence panel performance. This study developed and used a robust finite element model to investigate the effects of the three-dimensional density distribution and moisture variation on the out-of-plane thickness-swell (TS) of OSB panels. The model incorporated results of other independent studies, including studies on resin content and moisture effects on OSB. The model focused on TS since it is often considered to be a measure of panel durability. Although prediction of the out-of-plane TS under changing moisture conditions was the focus of this research, use of the model to investigate in-plane swell can be achieved by fully utilizing the other degrees of translation available in the developed model. The uniqueness of the developed model is its use of a three-dimensional (3D) density distribution matrix in capturing an OSB panel's composition.

LITERATURE REVIEW

When an OSB panel is formed under hydraulic pressing, a density gradient from a complex interaction between temperature, moisture, and gas pressure conditions within the formed mat results. In the thickness direction of the formed panel, the gradient is characterized by high-density surface layers and low-density core layers, but may take on many forms depending on manufacturing conditions and desired end-product attributes.

The vertical density gradient of flat-pressed panel products has been well documented by researchers and producers (Suchsland 1962; Wang and Winistorfer 2000). The strong relationship between panel density, compaction characteristics, and subsequent panel properties such as bending strength, dimensional stability, surface quality, edge machining, and fastener

performance, has made OSB density variation research critically important to manufacturers and researchers. Historically, the density profile has been measured using a gravimetric approach, but in the last decade, nondestructive nuclear and x-ray instruments have become the standard means of analysis (Wang 1986; Laufenberg 1986).

There are numerous published research reports that describe the correlation between a panel's vertical density profile (VDP) and panel properties. Some of the physical and mechanical properties that are influenced by density include: modulus of elasticity (MOE), E, and modulus of rupture (MOR) (Rice and Carey 1978), internal bond (Schulte and Frühwald 1996), TS through OSB thickness (Wang and Winistorfer 2003), tensile strength (Plath and Schnitzler 1974), tensile and compression strength through OSB thickness in the in-plane direction (Steidl et al. 2003), linear expansion (Suzuki and Miyamoto 1998), and torsion shear strength (Shen and Carroll 1970).

The horizontal density distribution (HDD), which is mainly dependent on furnish (wood flake), geometry and forming, is also of critical importance. As strands are formed into a mat, some areas in the panel have more strands overlapping than other areas. Suchsland (1962) described variations in the horizontal density as undesirable because differential swelling between areas of varying density could cause damaging internal stresses in a panel.

The objective of this paper is to detail the development of a finite element model, to show how a 3D density distribution matrix was formulated and applied, and to use the developed model to predict thickness-swell. Emphasis is placed on the stiffness matrix formulation, moisture loading, and determination of TS as a result of induced strain from moisture loading or a soak test.

EXPERIMENTAL PROCEDURE

Materials

Two southern pine (*Pinus spp.*) and two aspen (*Populus spp.*) commercial OSB panels were

used in this work. 150- × 150- × 18-mm test specimens were cut from the panels. The test specimens had an initial average moisture content of 2%, determined through oven-drying. The assumed resin type for these commercially obtained OSB samples was diphenyl methane diisocyanate (MDI). Previous tests indicated the selected panels had TS in the range of 3–16%. The soak test adopted for this research followed ASTM D1037-06 standards for evaluating TS for wood composites. The specimens, first coated on the bottom surface with a silicone water sealant, were allowed to dry over a 24-h period. The four edges and top surface were left unsealed to reflect modeling conditions. Thickness-swell measurements were made at times of 2, 4, 8, 16, and 24 h.

Measuring 3D spatial density distribution

Density distributions in the plane of test specimens, HDD, and distributions through the thickness of the specimens, VDP, were obtained with the aid of an X-ray densitometer (INSPEX X-ray Inspection System). The samples were exposed to X-ray attenuation prior to the soak test, first in the horizontal direction for the HDD, and then in the vertical (thickness) direction for the VDP. Attenuation data were collected at 400 pts/m. At a nominal thickness of 18 mm, seven data points were collected at 3-mm intervals through the thickness of the specimens. The density referred to in this work is used consistently to refer to the dry density.

FINITE ELEMENT MODEL

Model overview

The developed model accounts for resin content, moisture content, and moisture diffusion. The model is capable of including factors either not yet researched or not accounted for in the model's present form. Figure 1 is a flow chart of modules dedicated to performing tasks that affect the mechanical and physical performance of OSB. The modules or routines incorporated functions developed outside this research and

that reflect density relationships with resin and moisture content (MC), temperature, specific gravity, porosity, MOE, diffusivity, and sorption. Simulations of TS over a specified soak period, usually 24 h, are iteratively performed at efficient time steps with each cycle representing an increment in moisture loading. At the end of each incremental moisture loading cycle, updates to the panel's geometry, stiffness, density, MC, MOE, and stress levels are made at all nodes of the finite element mesh.

At present, only the thickness swell in the vertical direction is modeled, or the only degrees-of-freedom are displacements perpendicular to the panel. The same conceptual framework could be used to model linear expansion.

Model representation of an OSB specimen

Oriented strandboards are typically three-layered composites comprising a top, core, and bottom layer. The top and bottom layer strands are oriented in the same direction and the core layer is oriented in a perpendicular direction to the top and bottom layers. For the purposes of finite element modeling, seven nodal planes (Fig. 2) were defined through the model specimen thickness. The nodal planes were numbered Nodal Plane 1 (bottom surface) to Nodal Plane 7 (top surface). Nodal Plane 1 was fixed and the remaining nodal planes were free to translate in the thickness direction. The top, core, and bottom layers were each defined by two element layers in thickness direction. Twelve elements were used along the length and width of a specimen. Overall, the top, core, and bottom layers were each defined by 2 sub-layers of 144 elements or 288 elements per specimen layer. Evaluation of the specimen top, core, and bottom layers was performed at the nodes.

Model operation

The model flow chart represents a snapshot of an iterative simulation process or loading cycle. The model operation begins with a geometric construction of a test sample followed by a discretization or meshing process based on the de-

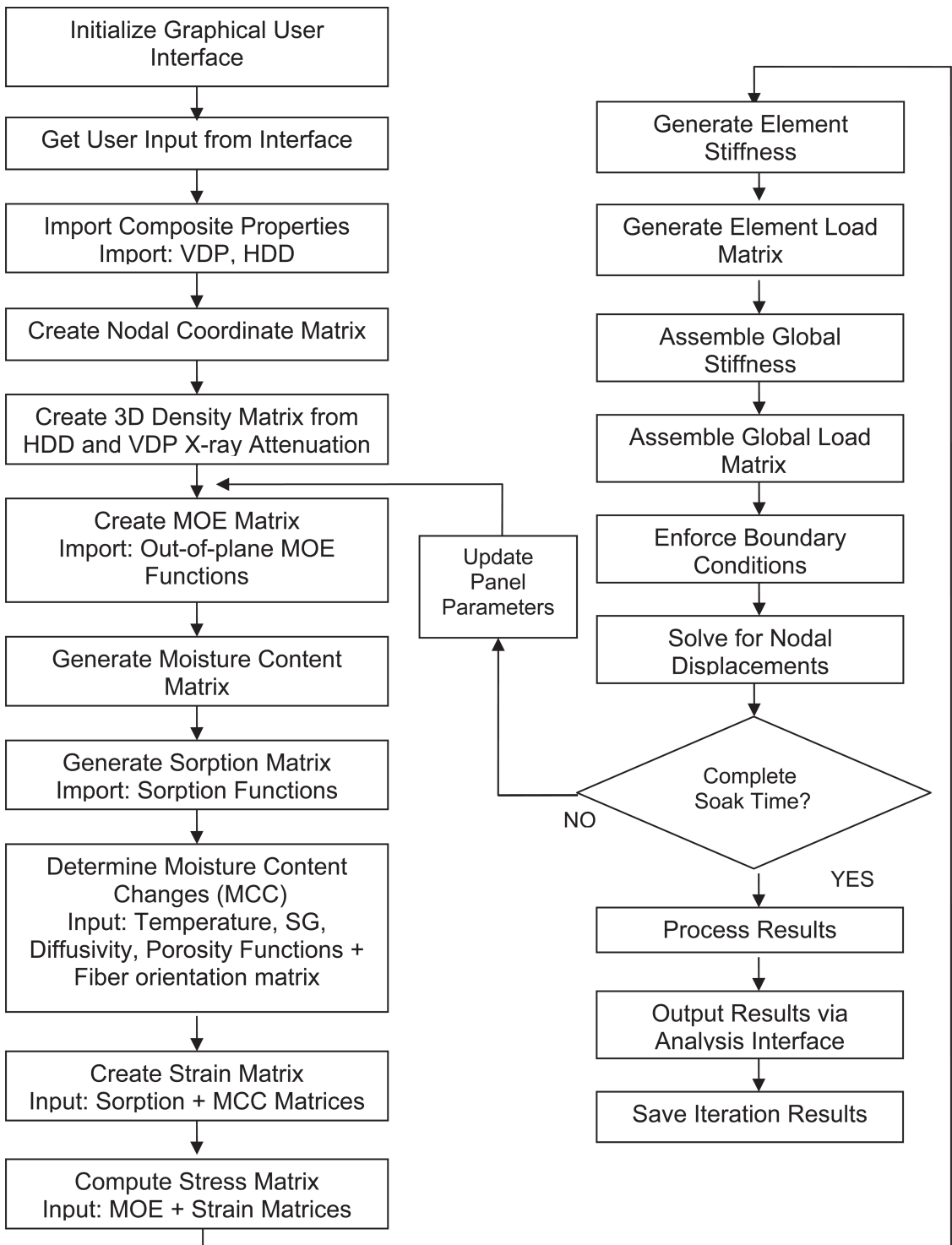


FIG. 1. Model flow chart.

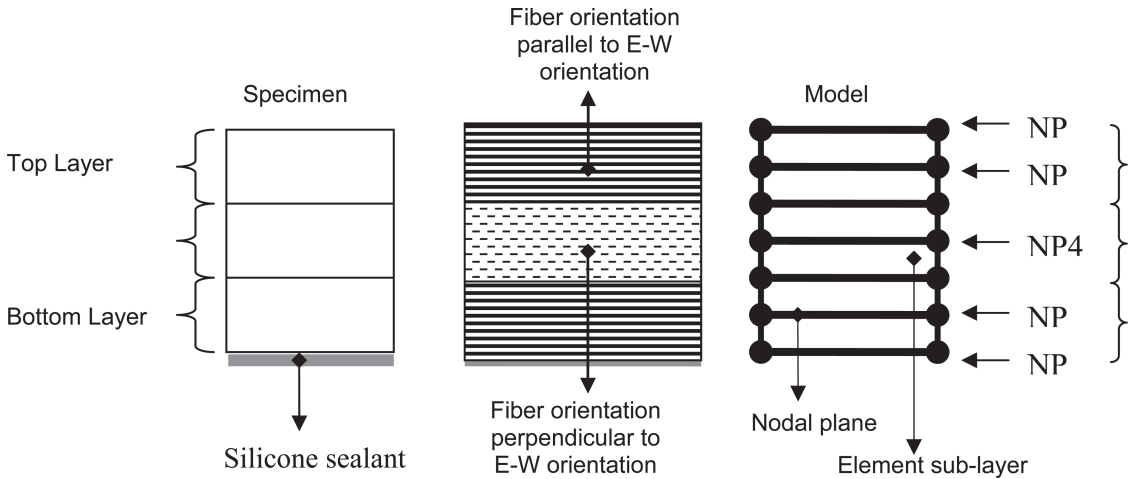


FIG. 2. Model representation of specimen layers.

sired mesh (finite element) size. This process is followed by a formulation of the 3D density matrix. Initialization matrices for the sample MC, resin fraction, and MOE based on nodal density are created.

From the specified ambient moisture conditions, ambient temperature, and initial MC, new nodal moisture contents are determined. The change in nodal strain is computed from the change in moisture content coupled with sorption data at the nodes. The out-of-plane MOE, either compression or tension, and newly computed nodal strain are used in calculating stresses at the nodes. Subsequent nodal stresses from additional strain are added to the previous iteration stresses.

The assembly of the panel stiffness and load matrices follow next. Boundary conditions of zero displacement in the out-of-plane direction were enforced for nodes in the bottom surface or lowest nodal plane and displacements at all other nodes solved for. Updates to the physical, mechanical, and geometric state of the model specimen were made at the nodes at the end of all iterations. The new nodal density at iteration N , ρ_N is evaluated as:

$$\rho_N = \frac{t_0}{t_N} [\rho_0] \quad (1)$$

where:

t_N = Thickness at a node at the end of iteration N (mm)

t_0 = Initial thickness at node (mm)

ρ_0 = Initial nodal density before moisture loading (kg/m^3)

Since sorption, stiffness, and load matrices are functions of density, any updates in panel nodal density result in updates of these parameters as well. When the soak time limit is reached, final model results are stored for post processing.

Element development

A specialized finite element code was written in MATLAB. Although several excellent general purpose finite element codes are available (e.g., ABAQUS, ANSYS, ADINA), there were advantages and reasons to develop our own code. The building unit of the modeled panel was the 8-noded brick element, Fig. 3, which generally has 3 degrees of freedom (d.o.f.) at a node. Although provisions for all three d.o.f. were made to facilitate future model expansion which would include displacements in the in-plane direction, the d.o.f. in this work was limited to translation in the thickness direction only. Also illustrated in Fig. 3 are the Gauss integration points. Displacements are shown for only the top nodes. By limiting the d.o.f., it was pos-

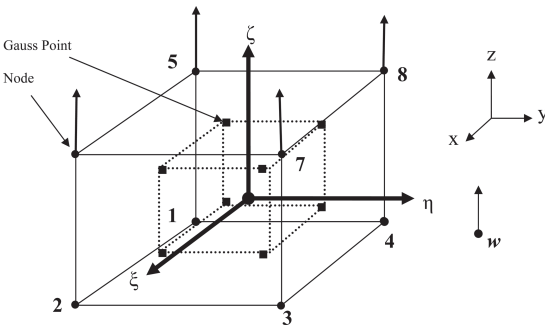


FIG. 3. Natural coordinates for the H8 element.

sible to avoid effects due to locking, a common problem with the general 8-noded brick (Cook 1995). The determination of displacements at the nodes was equivalent to determining TS.

The displacement in the z -direction, w , was determined using linear interpolation shape functions, f (Tackie 2006). The element stiffness matrix, k , for all elements was determined using virtual work, in which the integration was performed over the volume of the element. Since there is a nonlinear relationship between stress and strain and possible failure in tension, the integration required to obtain the element stiffness matrix cannot be performed in closed form, and numerical integration was required. For this work, $2 \times 2 \times 2$ Gaussian integration was chosen since Gaussian integration generally gives the most accurate numerical integration for a given number of points. The disadvantage of Gaussian integration is that there are no integration points on the surface of the element, which is often a place of interest.

The stiffness matrix, k , for the isoparametric hexahedron (H8 element) adopted for this work was formulated as follows (Weaver and Johnston 1984):

$$k = \int_v B^T E B \partial V = \sum_{k=1}^2 \sum_{j=1}^2 \sum_{i=1}^2 B^T(w) E B(w) J(w) \quad (2)$$

where: $B = df_i = 1 \times 8$ matrix relating strains to nodal displacements.

where:

$B = df_i = 1 \times 8$ matrix relating strains to nodal displacements.

$E = 1 \times 1$ constitutive matrix.

$J = D_L C_N = 1 \times 1$ jacobian matrix.

$C_N = 8 \times 1$ array of nodal coordinates of the H8 element.

$D_L = [f_{1\zeta} \ f_{2\zeta} \ f_{3\zeta} \ f_{4\zeta} \ f_{5\zeta} \ f_{6\zeta} \ f_{7\zeta} \ f_{8\zeta}]$

$f_{1i} = \frac{\partial f_i}{\partial \zeta}$ - Out-of-plane derivatives of

the shape functions.

The E matrix was obtained using Linville's (2000) empirical equations that relate MOE to density, resin fraction, and moisture content for MDI resin. The empirical equations reflect changes in the out-of-plane MOE at all nodes under compressive and tensile strains. The equations for the MOE in MPa are (Linville 2000):

$$\text{Compression: } E_C = 47.3 + 0.0114\rho + 1630R - 788M \quad (3)$$

$$\text{Tension: } E_T = A_T + B_T \epsilon_T \quad (4)$$

where: $A_T = 35.7 + 0.00632\rho + 1980R - 597M$

$$B_T = -A_T^2/615$$

$\epsilon_T =$ Tensile strain

$\rho =$ Density (kg/m^3)

$R =$ Resin fraction

$M =$ Percent moisture content (%)

The element stiffness matrices were assembled to form a global stiffness matrix, K , which represented the stiffness matrix for the entire sample and related applied panel forces, P , resulting from moisture induced strain to the displacements, U , at the nodes. By modeling displacement only in the through-the-thickness direction, it was possible to use a significant number of elements. A $150 \times 150 \times 18$ -mm thickness-swell sample was typically meshed with an element dimension of $12.5 \times 12.5 \times 3$ -mm, resulting in 864 elements. The element size was chosen based on an approximate representative volume. The size is small enough to cap-

ture density variations and behavior, yet large enough to represent the overall behavior of the OSB.

The uniqueness of the model was the ability to assign to all nodes different properties, such as density, MC, resin content (RC), and MOE, allowing the model to closely reflect local conditions in the panel. In a similar fashion, the load matrix, p_o was evaluated as follows:

$$p_o = \int_v B^T E \varepsilon_{TS} dV = \sum_{k=1}^2 \sum_{j=1}^2 \sum_{i=1}^2 B^T(w) E \varepsilon_{TS} J(w) \tag{5}$$

where: ε_{TS} = Matrix of nodal strains.

Spatial density matrix assembly

The initial 3D nodal density matrix needed to be assembled by combining the HDD and VDP. Each specimen's HDD acquired from X-ray attenuation was first divided as shown in the superimposed lettered and numbered grid in Fig. 4. Density assignment to grid intersections was achieved by averaging the horizontal density data of all attenuation points in the tributary areas surrounding the grid intersections. The at-

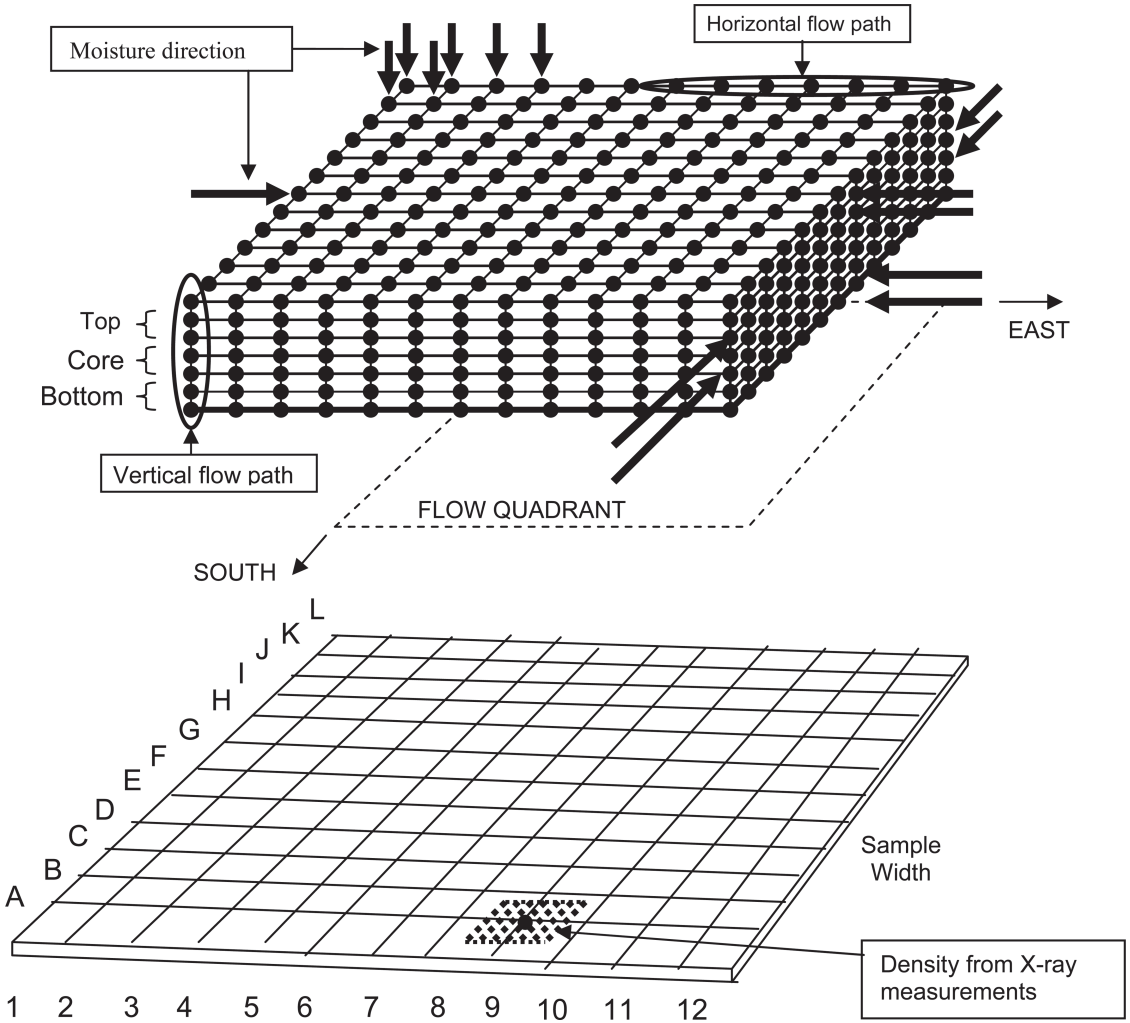


FIG. 4. Moisture flow paths and grid for HDD.

tenuation points within the tributary area for grid intersection A9 are shown in Fig. 4. For any node n with tributary area dimensions $a \times b$, and in a nodal plane p , the total number of nodes averaged was abm^2 , assuming the X-ray resolution was m data points per unit length. The mean horizontal nodal density ρ_{H}^{np} is given in Eq. (6).

$$\rho_{H}^{np} = \frac{\sum_{y=1}^{bm} \sum_{x=1}^{am} \rho_{x,y}}{abm^2} \text{ (kg/m}^3\text{)} \quad (6)$$

where:

$$\rho_{x,y} = \text{Density at point } (x, y) \text{ within tributary area } a \times b \text{ (kg/m}^3\text{)}$$

Twelve vertical density profiles were obtained, one each for sections A–L. Grid areas found in lettered grid sections were assumed to share the same VDP. In section-A for instance, grid areas A1–A12 shared the VDP for section A.

The 3D density matrix relied on the distribution of the mean horizontal nodal density ρ_{H}^{np} , in the thickness direction. A ratio of the mean layer vertical density to the overall mean of layer vertical densities in a given lettered grid section, J say, served as a weight for distributing ρ_{H}^{np} to discrete nodes in the thickness direction, Eq. (7).

$$\rho_v^{np} = \frac{\rho_P \times \rho_{H}^{np}}{\bar{\rho}_J} \text{ (kg/m}^3\text{)} \quad (7)$$

where:

- ρ_v^{np} = Vertically distributed mean horizontal nodal density to layer p in grid section J (kg/m³)
- $\bar{\rho}_J$ = Overall mean vertical density in grid section J (kg/m³)
- ρ_P = Mean layer vertical density in grid section J (kg/m³)

The series of vertically distributed, average horizontal densities defined the spatial density matrix. It was this spatial matrix that served as input for the finite element model.

Moisture content and loading

The loads exerted at the nodes result from swelling or shrinkage caused by gain or loss in

nodal moisture content. Linville (2000) showed that the induced strain, ϵ_{TS} , was linearly proportional to the change in moisture content.

$$\epsilon_{TS} = \beta \Delta M \quad (8)$$

where:

- β = $\rho[-0.00204R + 0.000255]$ = Swelling coefficient(%⁻¹)
- ρ = Density (kg/m³)
- R = Resin Fraction
- ΔM = Moisture content change (%)

The enforced boundary condition of the panel was fixity at nodal plane 1 (specimen bottom surface). This was analogous to laying the panel on a flat surface. The displacements at the nodes in all nodal planes were obtained using the global stiffness and load matrix. Since the material behavior and geometric changes of the panel under moisture-induced strain were nonlinear, an iterative approach was used in obtaining nodal displacements. The constitutive mechanical and physical properties, also functions of density, were reevaluated as changes occurred in the panel.

Mathematical formulation and discretization

The moisture-induced strain at a node was critical to the determination of nodal displacements. However, such strain required the solution of the moisture-stress-strain relation. The unsteady-state moisture transfer equation developed by Cloutier et al. (2001) for wood composites was used. The transverse diffusion coefficient, as given by Cloutier et al. (2001), is a function of the porosity of the wood, the average moisture content between nodes, the temperature, and the density. Implementation of the governing equations required a discretization process that also reflected physical changes in the sample as swelling occurred. The path that water may take in a wood composite can be influenced by factors such as porosity and fiber orientation. In order to reflect moisture movement in the composite, the discretization process required some simplification of the flow model. Figure 4 shows the adopted flow path of moisture as it

moved from the top surface to the lowest node and from the sides to the center of the panel. By sealing the bottom surface and leaving the remaining surfaces open, the model also reflected potential moisture exposure conditions in the field. Similar to the exposure conditions modeled here is the condition in which sheathing may be left unattended and exposed to the elements of weather before use. Horizontal flow in each model plane coincided with the corresponding layer's fiber orientation. For instance, if the surface layer's orientation was East-West (E-W), then the direction of flow was from the eastern edge of the specimen to the halfway point of the specimen in the E-W orientation and from the western edge of the specimen to the halfway point in the same E-W orientation. Flow in the core layer as a result was modeled North-South (N-S) to correspond to the fiber orientation of the core layer.

Although the equilibrium moisture content in wood composites is generally less than the fiber saturation point (FSP) of 30% in wood fibers, 30% was used as the upper bound for moisture at the nodes in the model. This limitation was imposed since there is limited knowledge of the effect of moisture on density beyond the FSP, and Eq. (8) is not valid beyond the FSP. Based on verification results presented in the next section, this limitation does not appear to significantly affect the model behavior.

A superposition of the flow paths, top to bottom and from the sides, contributed to the moisture content change at any given node. During each iterative process, the net moisture content was checked against the fiber saturation point, the point beyond which no further moisture content change was permitted. Partitioning the panel in this form aided the discretization process and made implementation into a computer program much more tractable. Solution of Cloutier's transient state moisture transfer equation was done using the method of lines for partial differential equations (Anderson 1995). At the exposed specimen surfaces where there is moisture exchange between the nodes and surroundings, the rate of moisture gain or loss was determined using an equation suggested by Geankoplis

(1993). From Eq. (8), the through-the-thickness strain due to moisture changes at the nodes, ϵ_{TS} , was computed. Nodal loads were computed using Eq. (5).

MODEL VERIFICATION

One sample from each of the four different panels was selected for model calibration. All samples had an initial moisture content of 2%, determined through oven-drying. It was assumed for all samples that the initial strain was zero as no moisture loading had taken place at time 0h. All nodes in the meshed panel were initialized to density values from the 3D density distribution matrix created from the HDD and VDP X-ray attenuation data. Initial MOE values were assigned to nodes based on the assigned nodal density, resin fraction, MC and Linville's (2000) out-of-plane tensile and compressive MOE equations, Eqs. (3) and (4). The moisture content at the exposed surfaces was taken as 30%, corresponding to 100% relative humidity conditions. The calibration samples were used to estimate the resin content of the samples, which was unknown for the commercial panels. The resin content determined from the calibration samples was used for the remaining samples from a given OSB panel.

An explicit 2nd order finite difference equation was employed in the solution of the transient moisture movement equation. The solution required an efficient, yet accurate, iteration time step. A normalized graph of thickness-swell prediction versus number of time steps was created, Fig. 5. To strike a balance between an acceptable predicted solution and the number of iterations required to achieve the solution, time-steps of 2 h or less were used. One sample from each panel type was used for calibration of resin content. Based on the calibrated resin content for the group representative sample and time step, TS predictions for the remaining samples were made and the results compared to experimental measurements.

RESULTS AND DISCUSSION

Figure 6 compares the experimental and predicted average swell over 24 h for one of the

Prediction (%TS with 48 time steps)

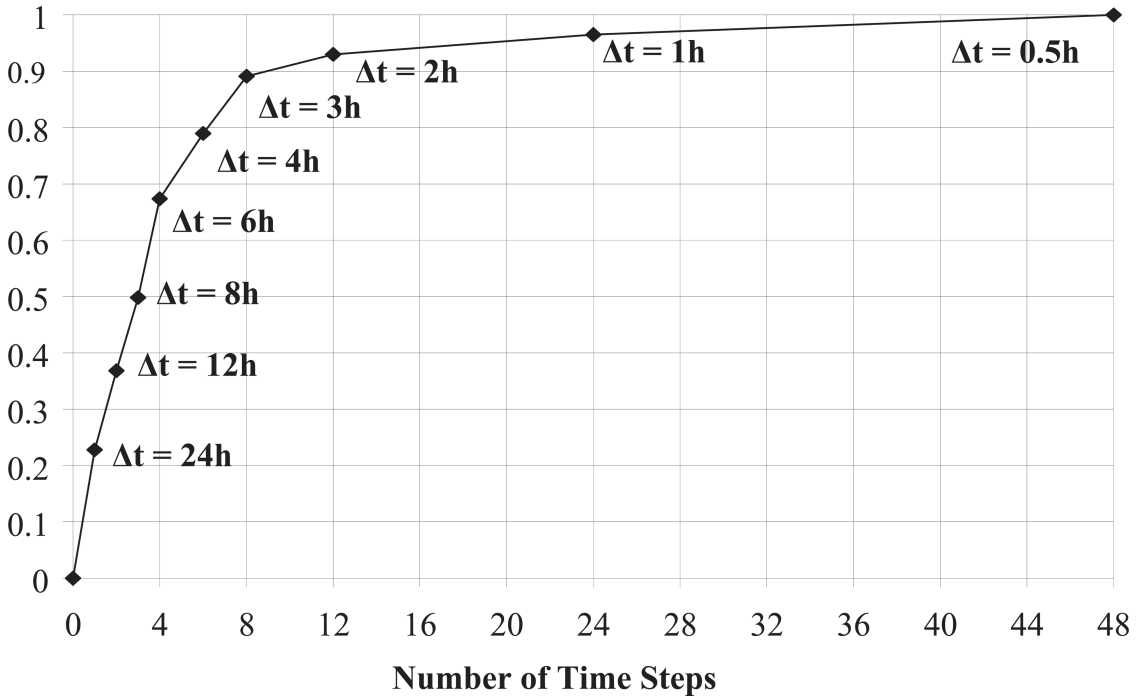


Fig. 5. Thickness-swell vs. number of iterations.

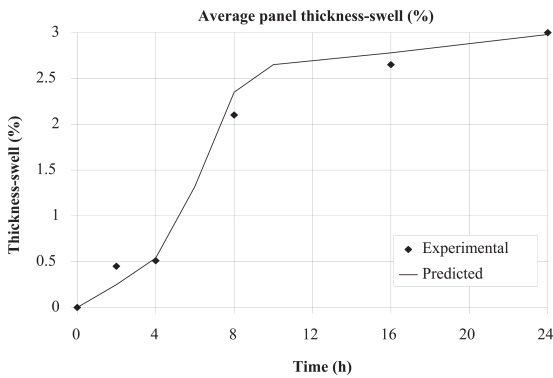


Fig. 6. Experimental vs. predicted average TS for Pine – Sample 1.

Fig. 6, the model predictions of layer TS are shown in Fig. 7, with the nodal planes being numbered from the bottom (sealed surface) to the top. This plot shows the models ability to show the internal behavior of the panel. For example, for this particular specimen there was large swell in the bottom layer, with less in the core and top layer. Very little thickness-swell occurred between nodal planes 5 and 6, the lower part of the top layer.

pine panels. The average swell is the average of the four midpoint TS measurements 25 mm from the sample edge. The results for all four panels are summarized in Table 1. The model favorably predicted 24-h TS for a range of TS in the two OSB types evaluated. For the same specimen in

CONCLUSIONS

Many aspects of OSB behavior, such as density variations, moisture flow, and constitutive properties, have been previously studied. The finite element model provides a means of integrating the results of these studies into a single model. As many of the behavioral aspects of OSB can be related to density, the developed model is based on the 3D density distribution.

TABLE 1. Experimental and predicted average percent TS of samples.

Time (h)		Experimental TS (%)					Predicted TS (%)		% Error
		0	2	4	8	16	24	24	
PINE 1	Sample 1	0	0.4	0.5	2	2.7	3	2.95	-1.7
	Sample 2	0	0.4	1	1.5	2.7	3.4	3.1	1.5
	Sample 3	0	0.5	1.3	0.8	2.4	3.3	3.25	-1.5
PINE 2	Sample 1	0	2.6	4.6	9.1	14.5	16.9	16	-5.3
	Sample 2	0	2.9	5.2	8.3	12.9	15.3	15.5	1.3
	Sample 3	0	2.5	4.1	7.6	13.2	16.9	15.75	-6.8
ASPEN 1	Sample 1	0	0.6	1.1	1.9	2.5	3.1	3	3.2
	Sample 2	0	0.4	1.1	1.4	2	3	3.1	3.3
	Sample 3	0	0.9	1.6	1.4	2.7	2.9	3.1	3.4
	Sample 4	0	0.3	1.1	1.1	2.5	3	3.2	6.9
ASPEN 2	Sample 1	0	0.5	1.2	1.7	3	4.1	4.75	15.9
	Sample 2	0	0.9	1.7	2.4	3.7	4.6	4.5	-2.2
	Sample 3	0	0.5	1.2	1.8	3.8	4.8	4.6	-4.2
	Sample 4	0	0.5	1.3	1.5	3.4	4.4	4.8	9.1

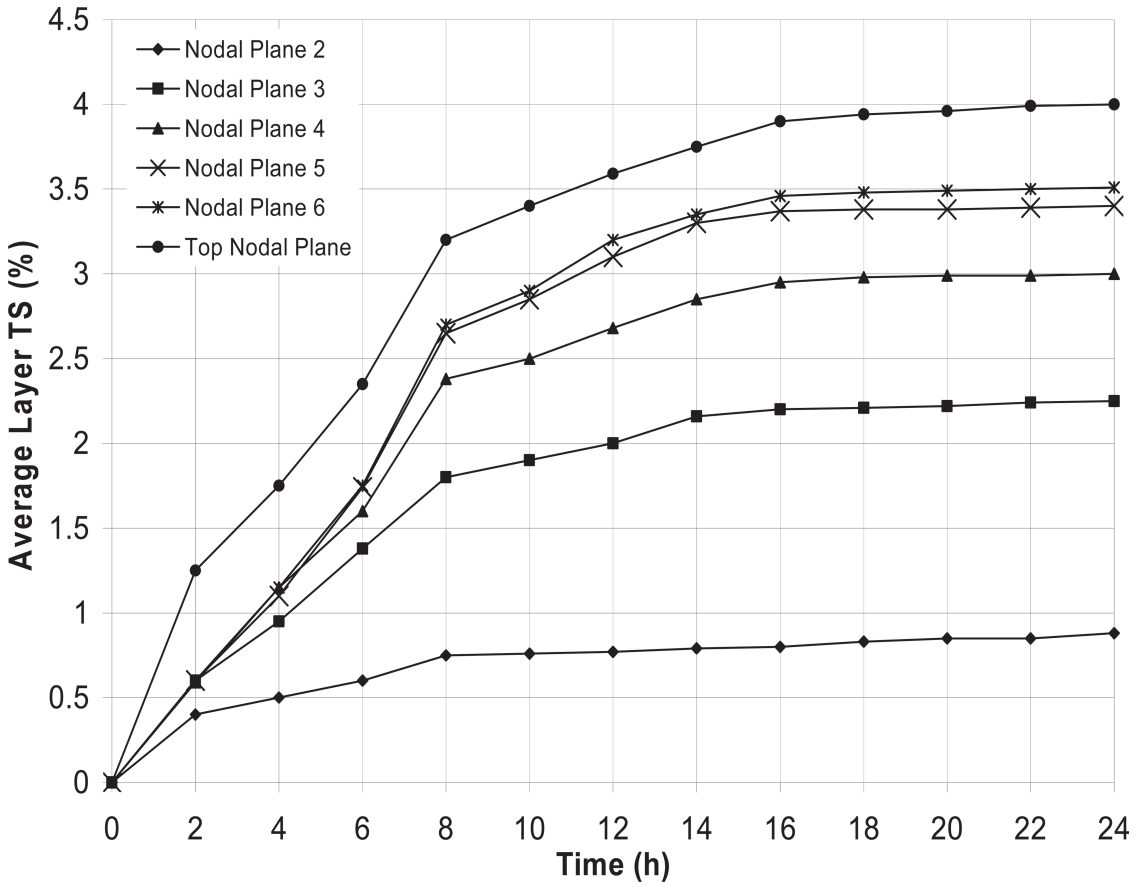


FIG. 7. Predicted average layer TS for Pine – Sample 1.

The model is initially used to predict thickness-swell, since that is a primary area of concern in OSB. The model was able to predict average thickness-swell of commercial panels with an acceptable error (generally less than 10%). Future papers will present results of parametric studies and the examination of internal stresses.

REFERENCES

- ANDERSON, J. D. 1995. Computational fluid dynamics: The basics with applications Mc Graw Hill, New York, NY.
- AMERICAN SOCIETY OF TESTING AND MATERIALS (ASTM). 2006. Standard Test Methods for Evaluating Properties of Wood-Base Fiber and Particle Panel Materials. D1037-06. American Society of Testing and Materials, West Conshohocken, PA.
- CLOUTIER, A., G. GENDRON, P. BLANCHET, AND R. BEAUREGARD, 2001. Finite element modeling of dimensional stability in layered wood composites. Pages 63-72 in Proc. 35th International Particleboard Composite Materials Symposium, April 2-5, 2001, Washington State University, Pullman, WA.
- COOK, R. D. 1995. Finite element modeling for stress analysis, John Wiley & Sons, New York, NY. 320 pp.
- GEANKOPLIS, C. J. 1993. Transport processes and unit operations. 3rd edition, Prentice Hall, Englewood Cliffs, NJ. 921 pp.
- LAUFENBERG T. L. 1986. Using gamma radiation to measure density gradients in reconstituted wood products. Forest Prod. J. 36(2):59-62.
- LINVILLE, J. D. 2000. The influence of a horizontal density distribution on moisture-related mechanical degradation of oriented strand composites. M.S. Thesis, Washington State University, Pullman, WA. 121 pp.
- PLATH, E., AND E. SCHNITZLER. 1974. The density profile, a criterion for evaluating particleboard. Holz Roh-Werkst. 32:443-449.
- RICE, J. T., AND R. H. CAREY. 1978. Wood density and board composition effects on phenolic resin bonded flakeboard. Forest Prod. J. 28(4):21-28.
- SCHULTE, M., AND A. FRÜHWALD. 1996. Shear modulus, internal bond and density profile of medium density fiber board (MDF). Holz Roh-Werkst. 54:49-55.
- SHEN, K. C., AND M. N. CARROLL. 1970. Measurement of layer strength distribution in particleboard. Forest Prod. J. 20(6):53-55.
- STEIDL, C. M., S. WANG, R. M. BENNETT, AND P. M. WINISTORFER. 2003. Tensile and compression properties through the thickness of oriented strandboard. Forest Prod. J. 53(6):72-80.
- SUCHSLAND, O. 1962. The density distribution of flakeboards. Michigan Agriculture Experiment Station. Quarterly Bulletin 45(1):104-121.
- SUZUKI, S., AND K. MIYAMOTO. 1998. Effect of manufacturing parameters on the linear expansion and density profile of particleboard. Wood Sci. 44:444-450.
- TACKIE, A. D. 2006. Determination of oriented strandboard properties from a 3D density distribution using the finite element method. Ph.D. dissertation, The University of Tennessee, Knoxville, TN. Pp. 39-44.
- WANG, S. 1986. A study and application of density gradient of wood-based panel. Science Report of Postgraduate 1(1):3-6 (In Chinese).
- , AND P. M. WINISTORFER. 2000. Fundamentals of vertical density profile formation in wood composites. Part 2. Methodology of vertical density formation under dynamic condition. Wood Fiber Sci. 32(2):220-238.
- , AND P. M. WINISTORFER. 2003. An optical technique for determination of layer thickness-swell of MDF and OSB. Forest Prod. J. 53(9):64-71.
- WEAVER, W., AND P. R. JOHNSTON. 1984. Finite elements for structural analysis. Prentice Hall, Inc., Englewood Cliffs, N.J. 03 pp.